Progress In Electromagnetics Research M, Vol. 26, 279–287, 2012

EFFECTS OF MICROWAVE FREQUENCY ON ELECTRON ENERGY DISTRIBUTION FUNCTION AND AIR BREAKDOWN USING THE FLUID MODEL

P. Zhao*, C. Liao, W. Lin, and J. Feng

Institute of Electromagnetics, Southwest Jiaotong University, Chengdu 610031, China

Abstract—The non-equilibrium electron energy distribution function (EEDF) obtained via solving the Boltzmann equation is introduced into the fluid model,and the effects of the microwave frequency on the EEDF and air breakdown are investigated. Numerical simulations show that the breakdown threshold of the fluid model with the non-equilibrium EEDF agrees well with that of the reported experiments. The microwave frequency plays an important role on the shape of the non-equilibrium EEDF at low pressures. The breakdown time at the low pressures predicted by the Maxwellian EEDF is shorter than that from the non-equilibrium EEDF in low-frequency oscillating fields, while matches the latter in high-frequency oscillating fields.

1. INTRODUCTION

The high power microwave (HPM) pulse has important applications in directed energy weapons, earth-space communications and the creation of artificial ionized layers in the atmosphere, etc. [1, 2]. Significant progress in the multi-giga-watt HPM pulse has been made in recent years [3–5]. When the amplitude of the HPM pulse is higher than the air breakdown threshold, the plasma produced by the ionization of air will attenuate and reflect the tail of the HPM pulse. Air breakdown has become one of major factors to limit the transmission and radiation of the HPM pulse.

Air breakdown caused by the HPM pulse has been studied by many investigators [6–9]. The fluid model with great advantages in simplicity and speed has been widely used in the simulation of the HPM breakdown in air [10–12]. In this fluid model, the electron

Received 12 October 2012, Accepted 31 October 2012, Scheduled 5 November 2012
* Corresponding author: Pengcheng Zhao (zhao_pc2010@163.com).

energy distribution function (EEDF), which is an important coefficient to calculate ionization parameters (ionization, attachment, collision and energy loss frequency), is often assumed to be a Maxwellian EEDF. After introducing the spherical harmonics expansion into the electron Boltzmann equation (BE), we can well know that the Maxwellian EEDF holds only when the collision frequency can be assumed constant [7]. However, the shape of the EEDF may depend on the microwave frequency if the collision frequency can not be assumed constant. Therefore, the Maxwellian EEDF can lead to inaccurate features of the air breakdown for different frequencies.

Resent work by Nam, et al. shows that the shape of the EEDF is weakly dependent on the microwave frequency at high pressure [7]. But at low pressure, the frequency can play an important role on the EEDF since it is comparable with or greater than the collision frequency. This problem as is known is still poorly understood especially for the fluid model.

A common method for finding the non-equilibrium EEDF is to solve the electron Boltzmann equation. Based on the classic two-term approximation, a user-friendly BE solver BOLSIG+ have been developed by [13]. The interaction of electron and molecule, i.e., elastic and all important inelastic collisions, is taken into account for calculating the EEDF in the BE solver.

In this paper, the non-equilibrium EEDF from BOLSIG+ is introduce into the fluid model, and the effects of the microwave frequency on the EEDF and air breakdown are investigated. In order to validate the accuracy of the non-equilibrium EEDF, we compare the air breakdown thresholds predicted by the fluid model with the non-equilibrium EEDF and the Maxwellian EEDF to the results from several experiments.

2. FLUID MODEL

The fluid model consists of Maxwell's equations, the electron fluid equations, as well as the ionization parameters which can be obtained by integrating the collision cross section over the electron energy distribution function.

2.1. Basic Equations

The basic equations for the one-dimensional fluid model are as follows [10]

$$\frac{\partial E_x}{\partial t} = -\left(\frac{1}{\varepsilon_0}\right)\frac{\partial H_y}{\partial z} - \frac{q_e U_x}{\varepsilon_0}, \tag{1}$$

$$\frac{\partial E_z}{\partial t} = -\frac{q_e U_z}{\varepsilon_0}, \tag{2}$$

$$\frac{\partial H_y}{\partial t} = -\left(\frac{1}{\mu_0}\right)\frac{\partial E_x}{\partial z}, \tag{3}$$

$$\frac{\partial N_e}{\partial t} = (\nu_i - \nu_a) N_e - \frac{\partial (N_e u_z)}{\partial z}, \tag{4}$$

$$\frac{\partial U_x}{\partial t} = \frac{q_e}{m_e} N_e E_x - \frac{q_e}{m_e}\mu_0 U_z H_y - \nu_c U_x, \tag{5}$$

$$\frac{\partial U_z}{\partial t} = \frac{q_e}{m_e} N_e E_z + \frac{q_e}{m_e}\mu_0 U_x H_y - \nu_c U_z - m_e \frac{\partial U_e}{\partial z}, \tag{6}$$

$$\frac{\partial U_e}{\partial t} = q_e (U_x E_x + U_z E_z) - \frac{\partial \overline{v}_z}{\partial z} U_e - N_e Q_l, \tag{7}$$

where E_x and E_z represent the electric field components along x-axis and z-axis, H_y is the magnetic component along y-axis. q_e and m_e denote the charge and mass of electron. ε_0 and μ_0 are the permittivity and permeability of free space. ν_i, ν_a, ν_c and Q_l are the ionization, attachment, collision and energy loss frequency of electron respectively. N_e denotes the free electron density. U_x and U_z are the components of the electron fluid velocity along x-axis and z-axis, U_e is the energy of the electron fluid. U_x, U_z and U_e can be written as

$$U_x = N_e \overline{v}_x, \quad U_z = N_e \overline{v}_z, \quad U_e = N_e \overline{\varepsilon}_e \ . \tag{8}$$

where $\overline{v}_x$ and $\overline{v}_z$ denote the mean electron velocity of the electron fluid along x-axis and z-axis, and $\overline{\varepsilon}_e$ denotes the mean electron energy.

2.2. Ionization Parameters

The ionization parameters are important to describe the interaction of the air molecules and the electrons accelerated by the microwave pulse, as shown in Eqs. (4)–(7). These parameters can be obtained as follows

$$\nu_j = N_{gas}\left[\int_0^\infty \sqrt{\frac{2\varepsilon_e}{m_e}}\sigma_j f(\varepsilon_e) d\varepsilon_e\right] \qquad (j = i, a, c), \tag{9}$$

$$Q_l = N_{gas}\left[\frac{8}{3\sqrt{\pi}}\frac{m_e}{M_{gas}}\int_0^\infty \sqrt{\frac{2\varepsilon_e}{m_e}}\sigma_c f(\varepsilon_e)\varepsilon_e d\varepsilon_e + \sum_{n,n\neq c}\int_0^\infty \sqrt{\frac{2\varepsilon_e}{m_e}}\sigma_n f(\varepsilon_e)\varepsilon_n d\varepsilon_e\right], \tag{10}$$

where M_{gas} and N_{gas} are the mass and density of the gas molecule respectively, $\sigma_{j,n}$ and ε_n represent the collision cross

section and threshold energy of each reaction set, and these cross sections for different gas have been experimentally and theoretically determined [14–16]. $f(\varepsilon)$ is the normalized EEDF. The detailed definition of the ionization parameters can be found in Ref. [9].

2.3. Electron Energy Distribution Function

The electron BE for the non-equilibrium assemble in an ionized gas is

$$\frac{\partial F}{\partial t} + \mathbf{v} \cdot \nabla F - \frac{q_e}{m_e}(\mathbf{E} + \mathbf{v} \times \mathbf{B}) \cdot \nabla_{\mathbf{v}} F = C[F], \tag{11}$$

where F is the electron distribution in six-dimensional phase space, and C represents the rate of change in F due to collisions. We employ the BE solver BOLSIG+, which takes into account of different growth models, quasi-stationary and oscillating fields and electron-neutral collisions [13], to obtain the non-equilibrium EEDF $f(\varepsilon)$ in Eqs. (9) and (10).

3. RESULTS AND DISCUSSIONS

The unknowns in Eqs. (1)–(7) are E_x, E_z, H_y, N_e, U_x, U_z and U_e, and we can employ the FDTD method to solve them [12]. Here, we assume that the air is composed of 21% oxygen, 78% nitrogen and 1% argon, in which there is a small number of seed electrons ($N_{e0} = 1.0\,\mathrm{cm}^{-3}$). The shape of the HPM oscillating field in time can be written as follow $E_i(t) = E_m \cdot \sin(2\pi f t)$, where E_m and f are the amplitude and frequency.

3.1. Comparison of Our Result and Experimental Data

Figure 1 shows the comparisons of the fluid model with the experiments at $f = 3.062\,\mathrm{GHz}$ and $110\,\mathrm{GHz}$ [17, 18], in which the pulse length t_p is 100 ns and 2500 ns respectively. The breakdown threshold is defined as the amplitude E_m when the electron density reaches the critical density N_{eb} for the air breakdown ($N_{eb} \approx 1.24 \times 10^{16} f^2_{\mathrm{GHz}}\,(\mathrm{m}^{-3})$) [19]. It can be seen from Fig. 1 that the breakdown threshold predicted by the fluid model with the non-equilibrium EEDF agrees well with the experimental results, while the Maxwellian EEDF gives lower breakdown threshold at high pressures and $f = 110\,\mathrm{GHz}$. This can be explained by the fact that the ionization frequencies based on the Maxwellian EEDF are larger than those from the non-equilibrium EEDF when the mean electron energy is low at the high pressures and high frequencies (detailed discussions see Subsection 3.2).

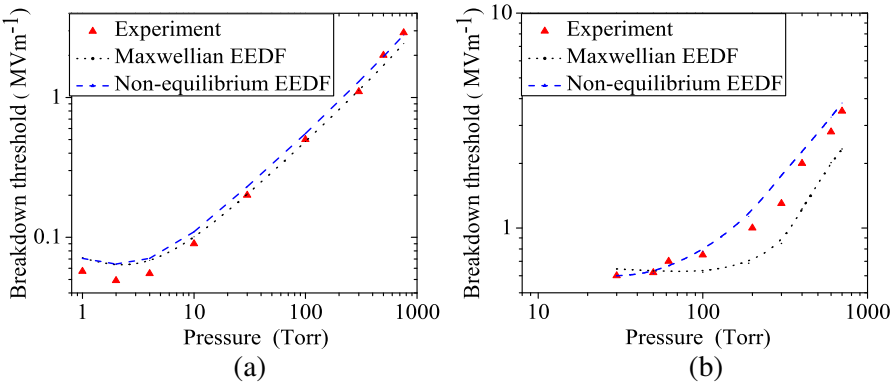

Figure 1. Comparisons of the air breakdown threshold between the experiments [17, 18], the fluid model with the Maxwellian EEDF and the non-equilibrium EEDF. (a) $f = 3.062\,\text{GHz}$ and $t_p = 100\,\text{ns}$. (b) $f = 110\,\text{GHz}$ and $t_p = 2500\,\text{ns}$.

3.2. Effect of the Frequency on the EEDF and Air Breakdown

We employ the BE solver BOLSIG+ to obtain the non-equilibrium EEDF with different mean electron energy $\overline{\varepsilon}_e$ for different microwave frequencies. As an example, Fig. 2 shows the comparisons of the Maxwellian EEDF with the non-equilibrium EEDF at 3 GHz and 110 GHz for $\overline{\varepsilon}_e = 4\,\text{eV}$. We can see from Fig. 2(a) that, at $p = 50\,\text{Torr}$, the Maxwellian EEDF can well approximate the non-equilibrium EEDF at 110 GHz, while its energy tail is much higher than that of the latter at 3 GHz. At $p = 500\,\text{Torr}$, no significant change takes place in the shape of the non-equilibrium EEDF as the frequency changes, and the energy tail of the Maxwellian EEDF is much higher than those of the non-equilibrium EEDF, as shown in Fig. 2(b).

Figure 3 shows the ionization frequencies as a function of $\overline{\varepsilon}_e$ based on the Maxwellian EEDF and the non-equilibrium EEDF. It can be seen from Fig. 3(a) that, at $p = 50\,\text{Torr}$, the Maxwellian EEDF predicts the ionization frequencies similar to those based on the non-equilibrium EEDF at $f = 110\,\text{GHz}$, but predicts larger ionization frequencies than the latter at 3 GHz, due to its higher energy tail (see Fig. 2(a)). From Fig. 3(b) we can see that, for $p = 500\,\text{Torr}$, the ionization frequency based on the Maxwellian EEDF is larger than those from the non-equilibrium EEDF at both $f = 3$ and 110 GHz, since the energy tail of the Maxwellian EEDF is overestimated (see Fig. 2(b)).

Figure 4 shows the breakdown time as a function of the frequency predicted by the fluid model with the Maxwellian EEDF and the non-

equilibrium EEDF at $\langle \bar{\varepsilon}_e \rangle = 4\,\text{eV}$ ($\langle\rangle$ represents the time average). Here the breakdown time is defined as the time in which the electron density reaches the critical density N_{eb} for the air breakdown. It can be seen from Fig. 4(a) that the breakdown time based on the Maxwellian EEDF is shorter than that from the non-equilibrium EEDF for low frequencies at $p = 50\,\text{Torr}$, but matches the latter for high frequencies. This is because the ionization frequency based on the Maxwellian EEDF is approximately equal to that from the non-equilibrium EEDF for high frequencies (see Fig. 3(a)).

In Fig. 4(b), the Maxwellian EEDF gives shorter breakdown

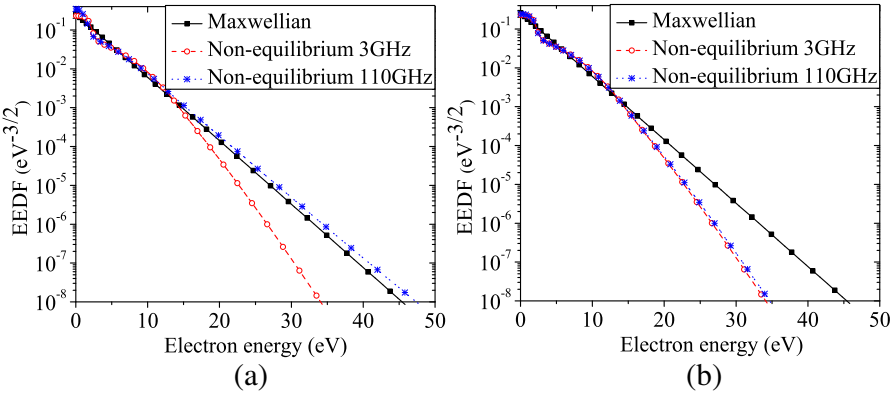

Figure 2. The Maxwellian EEDF and the non-equilibrium EEDF for different frequencies at $\bar{\varepsilon}_e = 4\,\text{eV}$. (a) $p = 50\,\text{Torr}$. (b) $p = 500\,\text{Torr}$.

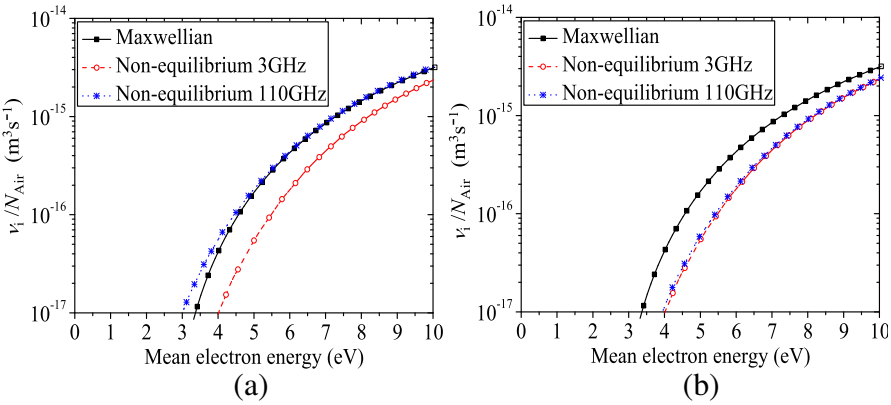

Figure 3. The ionization frequencies based on the Maxwellian EEDF and the non-equilibrium EEDF. (a) $p = 50\,\text{Torr}$. (b) $p = 500\,\text{Torr}$.

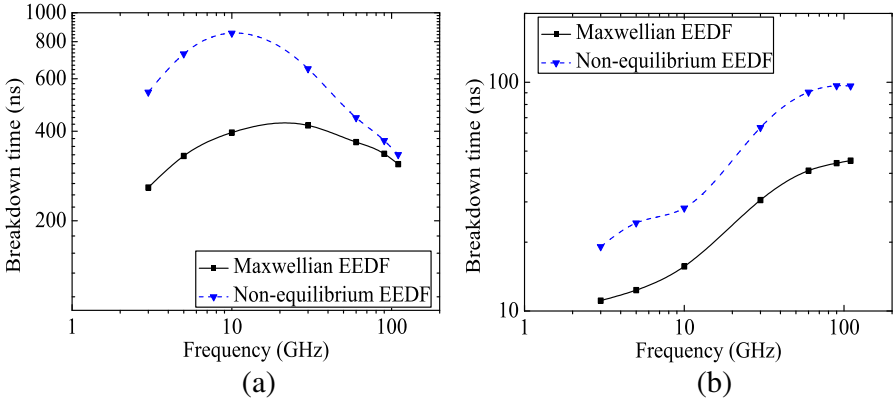

Figure 4. The breakdown time predictions as a function of the frequency for $\langle \bar{\varepsilon}_e \rangle = 4\,\text{eV}$. (a) $p = 50\,\text{Torr}$. (b) $p = 500\,\text{Torr}$.

time compared with the non-equilibrium EEDF over all frequencies at $p = 500\,\text{Torr}$, and this is because the energy tail of the Maxwellian EEDF is overestimated and leads to larger ionization frequencies, as shown in Fig. 2(b) and Fig. 3(b).

4. CONCLUSION

In this paper, the non-equilibrium EEDF obtained via solving the Boltzmann equation directly is introduced into the fluid model, and the effects of the microwave frequency on the EEDF and air breakdown are investigated when the mean electron energy is below 10 eV. The advantage of the non-equilibrium EEDF over the Maxwellian EEDF on the simulations of HPM breakdown in air is demonstrated with several experiments. Our simulation results show the breakdown time at low pressures predicted by the Maxwellian EEDF is shorter than that from the non-equilibrium EEDF in low-frequency oscillating fields, since the energy tail of Maxwellian EEDF is overestimated and generates larger ionization frequencies. However, the Maxwellian EEDF can well approximate the non-equilibrium EEDF for high frequencies at the low pressures, and the corresponding breakdown times are in agreement.

ACKNOWLEDGMENT

This work is supported by the Research Fund of Key Laboratory of HPM Technology (2012-LHWJJ.006), the Doctoral Fund of Ministry of Education of China (Grant No. 20110184110016), the Program for

New Century Excellent Talents in University of Ministry of Education of China (Grant No. NCET-10-0702), and the Open Research Fund of Key Laboratory of Cognitive Radio and Information Processing of Ministry of Education of China (Grant No. 2011KF05).

REFERENCES

1. Lofgen, M., D. Anderson, M. Lisak, and L. Lundgren, "Breakdown-induced distortion of high power microwave pulses in air," *Phys. Fluids B,* Vol. 3, No. 12, 3528–3531, 1991.
2. Nielsen, P. E., *Effect of Directed Energy Weapons,* Directed Energy Profession Society, New Mexico, 2009.
3. Wang, H., J. Li, H. Li, K. Xiao, and H. Chen, "Experimental study and spice simulation of cmos inverters latch-up effects due to high power microwave interference," *Progress In Electromagnetics Research,* Vol. 87, 313–330, 2008.
4. Kancleris, Z., G. Slekas, V. Tamosiunas, and M. Tamosiuniene, "Resistive sensor for high power microwave pulse measurement of Te01 mode in circular waveguide," *Progress In Electromagnetics Research,* Vol. 92, 267–280, 2009.
5. Chang, C., X. Zhu, G. Liu, J. Fang, R. Xiao, C. Chen, H. Shao, J. Li, H. Huang, Q. Zhang, and Z.-Q. Zhang, "Design and experiments of the GW high-power microwave feed horn," *Progress In Electromagnetics Research,* Vol. 101, 157–171, 2010.
6. Kim, J., S. P. Kuo, and P. Kossey, "Modelling and numerical simulation of microwave pulse propagation in an air-breakdown environment," *J. Plasma Phys.,* Vol. 53, No. 3, 253–266, 1995.
7. Nam, S. K. and J. P. Verboncoeur, "Global model for high power microwave breakdown at high pressure in air," *Computer Phys. Communications,* Vol. 180, 628–635, 2009.
8. Tang, T., C. Liao, and W. B. Lin, "Characteristics of analysis of repetition frequency high-power microwave pulses in atmosphere," *Progress In Electromagnetics Research M,* Vol. 14, 207–220, 2010.
9. Zhao, P., C. Liao, and W. Lin, "Numerical studies of the propagation of high-power damped sine microwave pulse in the atmosphere," *Journal of Electromagnetic Waves and Applications*, Vol. 25, Nos. 17–18, 2365–2378, 2011.
10. Yee, J. H., R. A. Alvarez, D. J. Mayhall, D. P. Byrne, and J. Degroot, "Theory of intense electromagnetic pulse propagation through the atmosphere," *Phys. Fluids,* Vol. 29, No. 4, 1238–1244, 1986.

11. Chaudhury, B. and J. Boeuf, "Computational studies of filamentary pattern formation in a high power microwave breakdown generated air plasma," *IEEE Trans. Plasma Sci.,* Vol. 38, No. 9, 2281–2288, 2010.
12. Zhao, P., C. Liao, W. Lin, C. Chang, and H. Fu, "Numerical studies of the high power microwave breakdown in gas using the fluid model with a modified electron energy distribution function," *Phys. Plasmas,* Vol. 18, 102111, 2011.
13. Hagelaar G. J. M. and L. C. Pitchford, "Solving the Boltzmann equation to obtain electron transport coefficients and rate coefficients for fluid models," *Plasma Sources Sci. Technol.,* Vol. 14, 722–733, 2005.
14. Vahedi, V. and M. Surendra, "A monte carlo collision model for the particle-in-cell method: Applications to argon and oxygen discharges," *Comput. Phys. Comm.,* Vol. 87, Nos. 1–2, 179–198, 1995.
15. Itikawa, Y., "Cross sections for electron collisions with nitrogen molecules," *J. Phys. Chem. Ref. Data,* Vol. 35, No. 1, 31–53, 2006.
16. Peterson, L. R. and J. E. Allen, "Electron impact cross sections for argon," *J. Chemical Phys.,* Vol. 56, No. 12, 6068–6076, 1972.
17. Tetenbaum, S. J., A. D. Macdonald, and H. W. Bandel, "Pulsed microwave breakdown of air from 1 to 1000 Torr," *J. Appl. Phys.,* Vol. 42, 5871–5872, 1971.
18. Cook, A., M. Shapiro, and R. Temkin, "Pressure dependence of plasma structure in microwave gas breakdown at 110 GHz," *Appl. Phys. Lett.,* Vol. 97, 011504, 2010.
19. Robert, R., "Optimization of HPM device parameters for maximum air transmission," *Intense Microwave Pulses,* Vol. 1872, 212–233, 1993.